Journal of Inflammation Research

Dovepress
Taylor & Francis Group

Open Access Full Text Article

ORIGINAL RESEARCH

Noninvasive Quantitative Evaluation of Proliferative Lupus Nephritis Based on Ultrasonic Viscoelastic Imaging

Han Yuan, Yuanyuan Chen, Liyan Wei, Xinhong Liao, Yong Gao

Department of Ultrasound, First Affiliated Hospital of Guangxi Medical University, Nanning, Guangxi, 530021, People's Republic of China

Correspondence: Yong Gao, Department of Ultrasound, First Affiliated Hospital of Guangxi Medical University, Nanning, Guangxi, 530021, People's Republic of China, Tel +86 15977486866, Email yonggaogx@163.com

Objective: To evaluate the role of ultrasonic viscoelastic imaging in predicting proliferative lupus nephritis (PLN).

Methods: We prospectively used ultrasonic viscoelastic imaging to evaluate 143 patients with lupus nephritis (LN), who underwent kidney biopsies from May 2023 to June 2024. Sixty healthy volunteers served as the control group. Patients were categorized as 90 cases of PLN, and 53 cases of nonproliferative lupus nephritis (nPLN). Ultrasonic viscoelastic imaging was employed to quantitatively analyze kidney cortex elasticity (Emean), viscosity coefficient (Vmean) and dispersion coefficient (Dmean). Semi-quantitative assessment of the lesion tissues was conducted based on the activity index and chronic index scoring system established by the National Institutes of Health (NIH) in 2018. The relationship among clinicopathological, conventional ultrasound factors and viscoelastic parameters was evaluated.

Results: Viscoelastic parameters (Emean, Vmean, and Dmean) significantly differed among the healthy control, PLN, and nPLN groups (all $p < 0.05$). The viscoelastic parameters (Emean, Vmean, and Dmean) of the PLN and nPLN groups exceeded those of the control group. Vmean and Dmean were considerably greater in the PLN group than in the nPLN group ($p < 0.05$). Vmean (OR 89.49, $p = 0.002$), serum creatinine (Scr) (OR 110.57, $p = 0.024$), and anti-dsDNA (OR 1.0, $p = 0.015$) were significant predictors of PLN. The combined model's area under curve (AUC) for predicting PLN was 0.83, better than any single indicator ($p < 0.05$). The peak systolic velocity (PSV) of the interlobar artery was determining factor of Emean ($p < 0.05$). The estimated glomerular filtration rate (eGFR), activity index, and body mass index (BMI) were determining factors of Dmean, while activity index was the determining factor of Vmean ($p < 0.05$). Correlation analysis reveals a positive correlation between Vmean and both the activity index and the chronicity index ($r = 0.57$ and $r = 0.34$, respectively, $p < 0.05$), as well as between Dmean and both the activity index and the chronicity index ($r = 0.43$ and $r = 0.20$, respectively, $p < 0.05$).

Conclusion: As a noninvasive examination method, ultrasonic viscoelastic imaging is beneficial for identifying PLN.

Keywords: viscosity, elasticity, lupus nephritis, proliferative lupus nephritis, active index, chronic index

Introduction

Multiple system inflammation is a hallmark of the chronic inflammatory disease known as systemic lupus erythematosus (SLE).[1] Lupus nephritis (LN) is a severe organ manifestation of SLE that is associated with major morbidity and death in SLE patients, with up to 20% of LN patients developing end-stage kidney disease.[2,3]

The pathology and pathologic type of LN underpin the choice of treatment and prognosis for patients. According to the International Society of Nephrology/Society of Renal Pathology (2003 ISN/RPS), the LN pathological types are divided into six categories, with types III, IV, and III/IV+V associated with capillary cell proliferation and defined as proliferative lupus nephritis (PLN), and types I, II, and V defined as nonproliferative lupus nephritis (nPLN).[4,5] Compared with nPLN, PLN has severe clinical manifestations and poor prognoses, requiring high-intensity immunosuppressive therapy.[6–8] The pathological mechanism of LN involves the deposition of immune complexes, which trigger a cascade of inflammatory reactions, ultimately leading to kidney damage and fibrosis.[3] Compared to nPLN, PLN is

Received: 3 December 2024
Accepted: 27 February 2025
Published: 6 March 2025

highly inflammatory, involving the deposition of immune complexes beneath the endothelium, accompanied by crescent formation and damage to the glomerulus and interstitium.[3,9,10] The most reliable method for identifying the disease type and activity of LN is a kidney biopsy.[4] Kidney biopsy is invasive procedure. However, it has specific risks, such as bleeding, infection, arteriovenous fistulas, and so on, especially in SLE patients. Hemorrhagic complications are relatively high, and about 7% of kidney biopsies still have serious complications.[11] Therefore, it is vital to develop new noninvasive methods for the early identification of PLN.

Ultrasound shear wave elastography (SWE) is a convenient, noninvasive technology for quantitatively assessing tissue elasticity, and it has significant potential for the evaluation of glomerular diseases and kidney function.[12,13] The principle behind SWE is that the tissue being imaged is uniformly elastic, meaning that a simple linear formula can be used to quantitatively assess tissue elasticity.[14] However, the liver and kidneys, which are organs with a rich blood supply, possess both elastic and viscous properties.[15,16] Therefore, relying solely on elasticity values for assessment may lead to unreliable results. Ultrasound viscoelastic imaging—a relatively new elastography technique—can be used to quantify simultaneously both the elasticity and viscosity of tissues. It has been used to evaluate diffuse liver diseases, diffuse thyroid diseases, glomerular diseases, and breast diseases.[17–20] Studies have shown that elasticity is superior to viscosity for evaluating fibrosis, although viscosity is superior to elasticity for assessing degrees of inflammation and necrosis.[21] In our previous study on the assessment of chronic kidney disease (CKD) using ultrasound viscoelastic imaging, we found that viscoelastic parameters had good diagnostic efficacy in predicting CKD and could also differentiate between different stages of CKD.[22]

In this study, we aimed to assess the effectiveness of ultrasonic viscoelastic imaging for detecting PLN by evaluating kidney tissue viscoelasticity.

Materials and Methods

Patients

This prospective study conformed to the Declaration of Helsinki and was reviewed and approved by the Medical Ethics Committee of the First Affiliated Hospital of Guangxi Medical University (Approval Number: 2023-K093-01). Patients with LN were enrolled from May 2023 to June 2024 and signed informed consent forms. The inclusion criteria were as follows: 1) age ≥ 14 years, 2) LN confirmed by kidney biopsy, and 3) submitted for ultrasound and viscoelastic imaging examination within 3 days prior to kidney biopsy. Patients with grade VI LN were excluded from this study due to distinct outcomes and clinical features. The exclusion criteria were as follows: 1) the presence of other diseases that might affect kidney viscoelasticity, such as kidney injury, kidney cyst, kidney tumor, and so on; 2) kidney artery stenosis or compression of the left kidney vein; 3) inadequate image quality control; and 4) at least 10 glomeruli in the optical microscope specimen.

In addition, we prospectively recruited 60 healthy people without kidney disease, hypertension, or diabetes, matched to the patient group's gender and age, to serve as the control group. Figure 1 shows the flowchart for this study.

Clinical Information

Patient data included demographic characteristics (sex, age, and BMI), liquid biopsy indicators (serum creatinine [Scr], C3, C4, and anti-dsDNA), and estimated glomerular filtration rate (eGFR) calculated using a CKD-EPI creatinine equation.[23] Liquid biopsy indicators were assessed within one week prior to kidney biopsy.

Conventional Ultrasound and Ultrasonic Viscoelastic Imaging

A Mindray ultrasound system (Resona R9, Mindray Bio-Medical Electronics Co, China) was used, equipped with viscoelasticity imaging software (4.1.0, Rev. 179255), a C5-1 transducer, and a frequency range of 1–5 MHz. An experienced sonographer with 10 years of experience, blinded to patients' clinical information, conducted consistent ultrasound examinations. Since all kidney biopsies in our center were performed on the left kidney, patients underwent conventional ultrasound and viscoelastic imaging of the left kidney in the lateral recumbent position after voiding. Multiparameter ultrasound measurements were performed on the maximum longitudinal plane of the kidneys.

After the images were stabilized, the viscoelastic imaging function was activated. During the operation, the probe was positioned vertically and firmly pressed against the skin without applying undue pressure. The sampling frame was

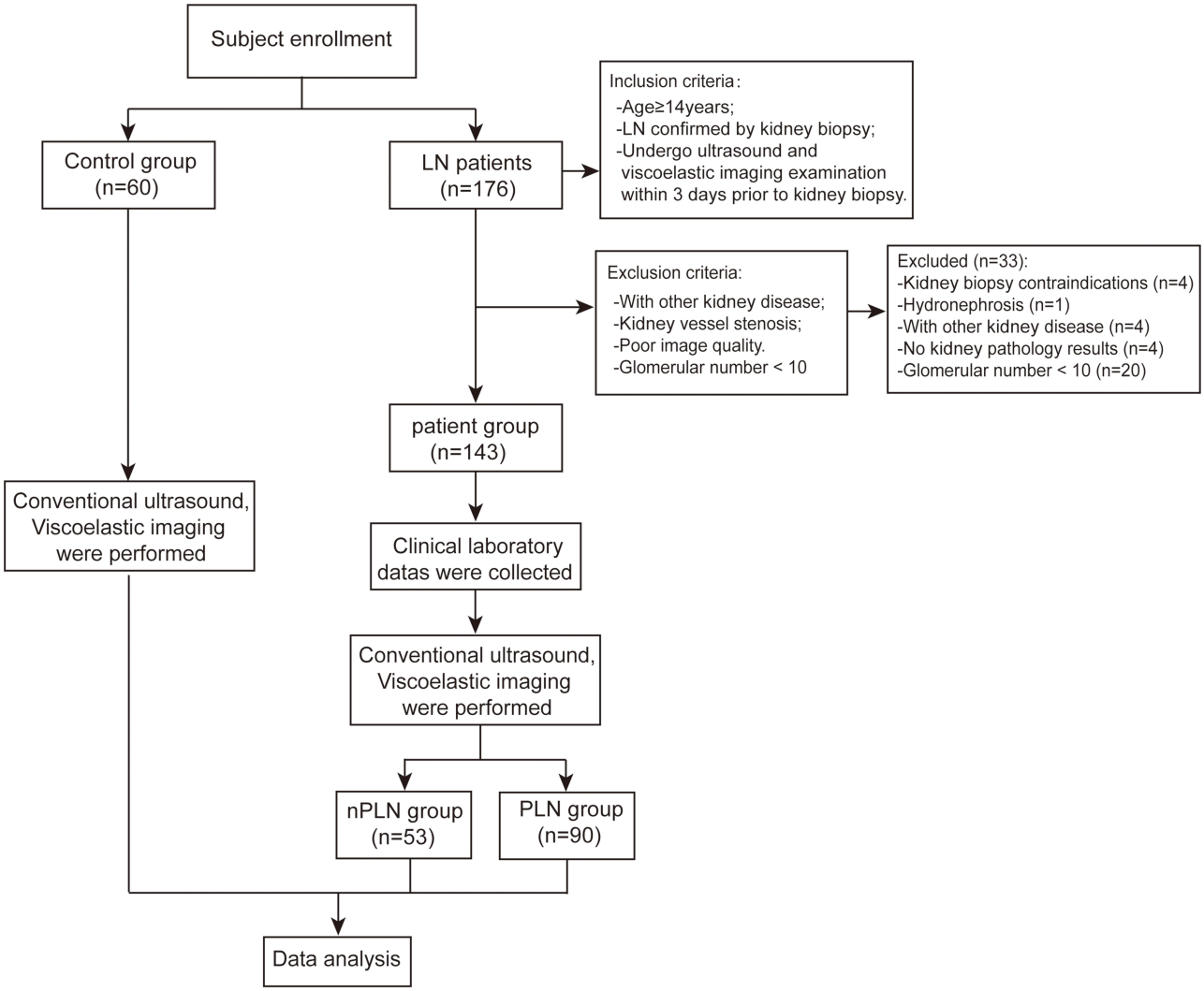

Figure 1 Flowchart of the research design.

positioned over the parenchymal area in the middle of the kidney, and viscoelasticity was measured while the patients held their breath. Subsequently, a quantitative sampling box (Qbox) with dimensions of 1 cm was used to collect data from the kidney cortex below the renal capsule (see Supplementary Figure 1). The average of at least five consecutive measurements was taken as the final result. The Qbox viscoelastic imaging system automatically calculated Young's modulus, viscosity coefficient, and dispersion coefficient. Emean denoted the average elasticity (kPa) of the tissue in the Qbox, Vmean referred to the average viscosity coefficient (Pa·s), and Dmean represented the average dispersion coefficient (m/s/kHz) (see Supplementary Figure 2).

Viscoelastic imaging facilitates simultaneous SWE imaging, reliability mapping, viscosity imaging, and dispersion imaging. SWE is used to quantitatively assess the stiffness of tissues based on the equation $E = 3\rho V^2$, where E stands for the hardness of the tissue, ρ represents the density, and V is the estimated shear wave velocity.[24] Shear wave dispersion imaging simplifies frequency-related changes in shear wave velocity into simple linear relationships, thereby allowing the indirect calculation of tissue viscosity.[16] Viscosity imaging, on the other hand, employs the Voigt model and thus more complex equations to interpret frequency-dependent changes in velocity, which facilitates a more accurate assessment of tissue viscosity.[20] Detailed information about viscosity imaging is contained in the Supplementary content.

https://doi.org/10.2147/JIR.S505223

We employed the following quality control standards for this study: each image should have 1) uniform color saturation and a moving stability index rating of three stars or higher, 2) a reliability index of 90% or above, and 3) an interquartile range (IQR)-to-median ratio not exceeding 30%.

To assess interobserver consistency, we randomly selected 20 participants from the study population, and two senior physicians who had received training in viscoelastic technology conducted the measurements. To ensure intraobserver consistency, Physician A repeated the measurements for these 20 participants one week later. Physician A conducted the measurements for all remaining patients. Finally, the viscoelasticity measurement data were calculated based on Physician A's measurements.

Kidney Biopsy and Histopathology

A kidney biopsy was conducted within three days of elastography, with ultrasound guidance and an 18G needle targeting the lower pole parenchyma of the left kidney. Two cores of kidney tissue were extracted, fixed in 10% formalin, and subsequently sent for histopathological analysis. Paraffin slices were analyzed using hematoxylin and eosin, periodic acid Schiff, and Masson's trichrome staining.

According to the 2003 ISN/RPS pathological classification standard, we divided LN patients into PLN and nPLN groups[5] and scored the pathological tissues using the National Institutes of Health activity index and chronicity index scores.[9] The LN activity index comprises six indicators: capillary endotheliosis, cellulosic necrosis and/or nuclear breakage, cellular crescent, hyaline thrombus or platinum ear change, leukocyte infiltration, and tubulointerstitial inflammation.[9] We assessed the parameters individually and categorized glomerular involvement as 0%, 1–24%, 25–50%, or > 50%, with a semiquantitative score of 0–3 points and a total possible score of 24.[9] The chronicity index facilitates semi-quantitative scoring based on glomerular sclerosis, fibrous crescents in glomeruli, cortical interstitial fibrosis, and cortical tubular atrophy, each of which was assigned 0–3 points, leading to a total possible score of 12 points.[9]

Statistical Analysis

We performed statistical analysis using SPSS® (version 26.0) and MedCalc software (version 20.0; MedCalc), presenting normally distributed data as mean ± standard deviation (SD). We used an independent samples *t*-test for group comparisons and employed a one-way analysis of variance (ANOVA) and a least significant difference (LSD) multiple comparison test to compare multiple groups. Nonnormally distributed data were presented as medians and IQRs, and we used the Mann–Whitney *U*-test and Kruskal–Wallis test to compare the groups. We identified independent factors influencing viscoelastic parameters and predicting PLN using both univariate and multivariate analysis. We evaluated diagnostic performance according to the receiver operating characteristic (ROC) curve, and we used the DeLong test to compare the diagnostic performance of different parameters. A p value of 0.05 was considered statistically significant.

Results

Cohort Characteristics

For this study, we continuously enrolled 176 LN patients who underwent kidney biopsies at our center. We excluded patients with renal biopsy contraindications (n = 4), hydronephrosis (n = 1), LN coexisting with other kidney diseases (n = 4), unclear pathological diagnoses (n = 4), and any patients with less than 10 punctured glomeruli (n = 20). Finally, 143 LN patients (mean age 33.3 ± 13.4 years; 127 females, 16 males) and 60 volunteers (mean age 35.6 ± 11.6 years; 51 females, 9 males) were included in the study. Table 1 summarizes the participants' demographic characteristics. Of the 143 patients, 90 (62.9%) were diagnosed with PLN, and 53 (37.1%) were diagnosed with nPLN. Supplementary Table 1 presents the patients' pathological information.

Clinical Parameters

The clinical parameters of the PLN and nPLN groups are shown in Supplementary Table 2. There were significant differences in Scr, anti-dsDNA, and eGFR between the groups (all $p < 0.05$).

Table 1 Baseline Data and Multi-Parameter Ultrasound of the Study Subjects

Characteristic	Control Group (n = 60)	nPLN Group (n = 53)	PLN Group (n = 90)	*p*
Years	33.5 (26.0–43.5)	32.0 (24.0–42.0)	30 (22.0–39.3)	0.196
Sex				0.458
Female	51 (85.0%)	49 (92.5%)	80 (88.9%)	
Male	9 (15.0%)	4 (7.5%)	10 (11.0%)	
BMI (kg/m^2)	21.8 (20.0–23.1)	20.4 (19.0–22.9)	22.2 (20.0–24.5)	0.057
Kidney length (cm)	10.36 ± 0.73	10.30 ± 0.87	10.47 ± 0.95	0.496
PSV of interlobar artery (cm/s)	28.96 ± 4.66	27.78 ± 5.32	26.76 ± 5.43[a]	0.029
RI of interlobar artery	0.51 ± 0.04	0.50 ± 0.05	0.50 ± 0.05	0.256
Emean (kPa)	5.77 ± 0.95	6.94 ± 1.77[a]	7.18 ± 2.26[a]	< 0.001
Vmean (Pa·s)	1.71 ± 0.14	2.02 ± 0.21[a]	2.27 ± 0.31[ab]	< 0.001
Dmean (m/s/kHz)	6.74 ± 0.65	7.67 ± 0.94[a]	8.22 ± 0.97[ab]	< 0.001

Notes: [a]Least significant difference test, compared to control group, $p < 0.05$. [b]Least significant difference test, compared to nPLN group, $p < 0.05$.

Conventional Ultrasound and Viscoelastic Imaging

Table 1 shows the conventional ultrasound and viscoelastic parameters of the control, nPLN, and PLN groups. The peak systolic velocities (PSV) of the interlobar kidney arteries differed significantly across the three groups ($p = 0.029$). Pairwise comparison revealed that the PSV in the PLN group was lower than that in the control group ($p < 0.05$). The viscoelastic parameters in the PLN and nPLN groups were significantly greater than those in the control group ($p < 0.05$). The Vmean and Dmean values in the PLN group were significantly greater than those in the nPLN group ($p < 0.05$), whereas the Emean values did not differ significantly between the groups ($p > 0.05$). Figures 2 and 3 illustrate representative cases.

Diagnostic Performance of Factors for Identifying PLN

Table 2 outlines the factors linked to PLN. Vmean, Dmean, Scr, Anti-dsDNA, and eGFR were significantly associated with PLN in the univariable analysis (all $p < 0.05$). The multivariate analysis determined that Vmean, Scr, and anti-dsDNA were determining factors for predicting PLN (all $p < 0.05$). We then combined these factors to construct a combined model.

Table 3 summarizes the diagnostic performance of independent influencing factors in distinguishing between PLN and nPLN. The AUC for Vmean for diagnosing PLN was 0.77, the sensitivity was 56.7%, and the specificity was 86.8%, with a cut-off value of 2.16 Pa·s. Using a combined Vmean, Scr, and anti-dsDNA model, the AUC increased to 0.83 (Figure 4). Applying a probability threshold of 0.66 as the cut-off value improved the sensitivity to 66.89% compared to Vmean alone.

Factors Associated With Viscoelastic Parameters

Table 4 summarizes the factors associated with Vmean. Through univariate and multivariate analysis, we found that only the activity index was a determining factor for the Vmean value ($p < 0.05$). Spearman correlation analysis showed that there was a significant moderate positive correlation between the activity index and Vmean ($r = 0.57$, $p < 0.001$).

Table 5 summarizes the factors associated with Dmean. Through univariate and multivariate analysis, we found that eGFR, BMI, and the activity index were the determining factors for the Dmean value (all $p < 0.05$). Spearman correlation analysis showed that BMI ($r = 0.25$, $p = 0.003$) and the activity index ($r = 0.43$, $p <0$ 0.001) had positive correlations with Dmean, while eGFR ($r = -0.44$, $p < 0.001$) had a negative correlation with Dmean.

Table 6 summarizes the factors associated with Emean. Through univariate and multivariate analysis, we found that the PSV of the interlobar artery was the determining factor for the Emean value ($p < 0.05$). Spearman correlation analysis revealed a positive correlation between the two variables ($r = 0.17$, $p = 0.046$).

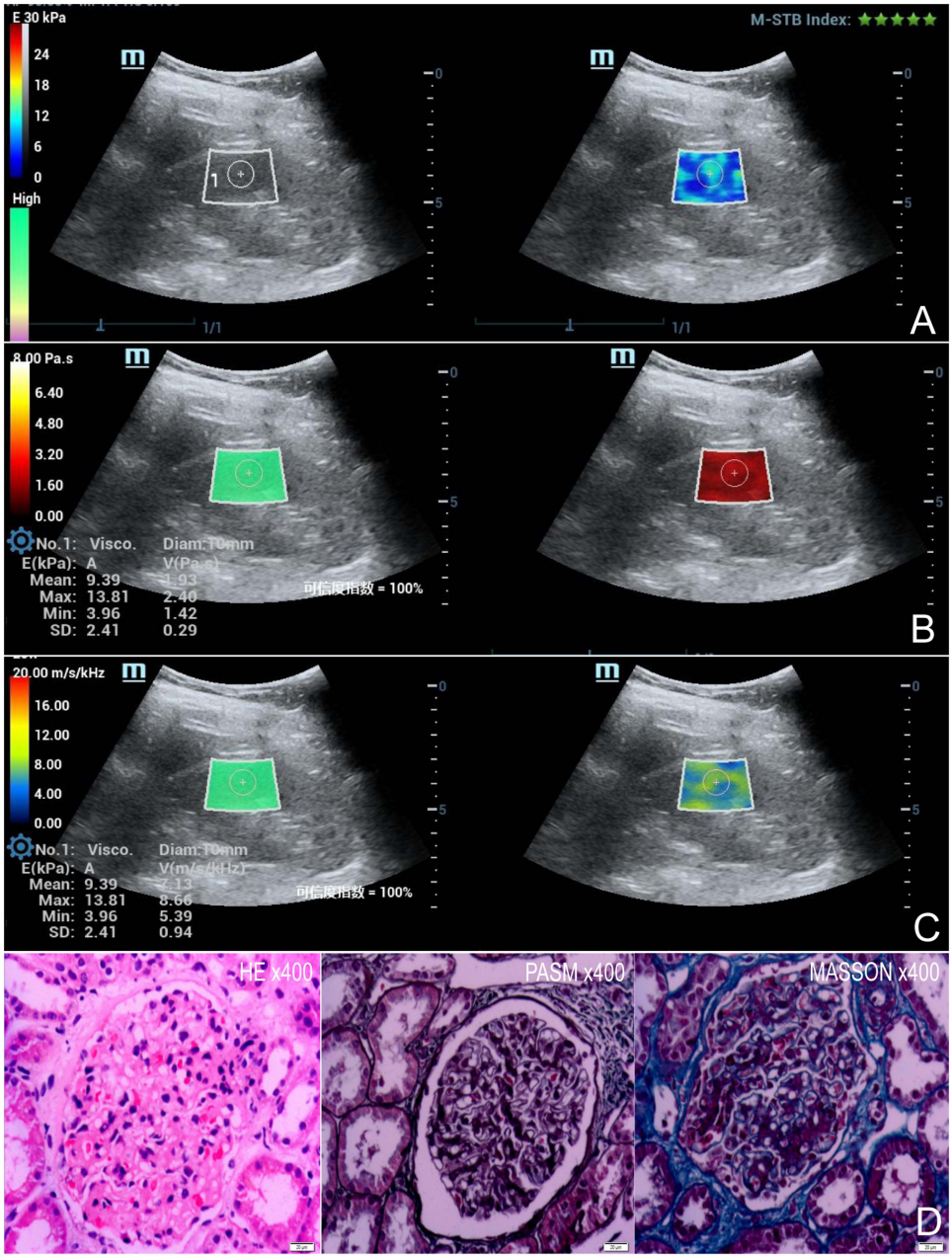

Figure 2 The pathological results were classified as nonproliferative lupus nephritis of type I according to ISN/RPS. (**A**) Conventional ultrasound showed that the echo of the renal parenchyma was uniform. The mean stiffness measured by viscoelasticity was 7.05 kPa. (**B**) The mean viscosity coefficient measured by viscoelasticity was 1.95 Pa·s. (**C**). The mean dispersion coefficient measured by viscoelasticity was 6.70 m/s/kHz. (**D**) HE staining, PASM staining, and MASSON staining of renal pathology.

Intergroup and Intragroup Consistency Analyses

The intraobserver consistency values for Emean, Vmean, and Dmean were 0.97 (95% CI: 0.94–0.99), 0.89 (95% CI: 0.76–0.96), and 0.95 (95% CI: 0.88–0.98), respectively. The interobserver consistency values for Emean, Vmean, and Dmean were 0.93 (95% CI: 0.82–0.97), 0.84 (95% CI: 0.65–0.93), and 0.87 (95% CI: 0.70–0.95), respectively.

Correlation Analysis

The correlation between viscoelastic parameters (Emean, Vmean, and Dmean) and pathological parameters were presented in Supplementary Table 3.

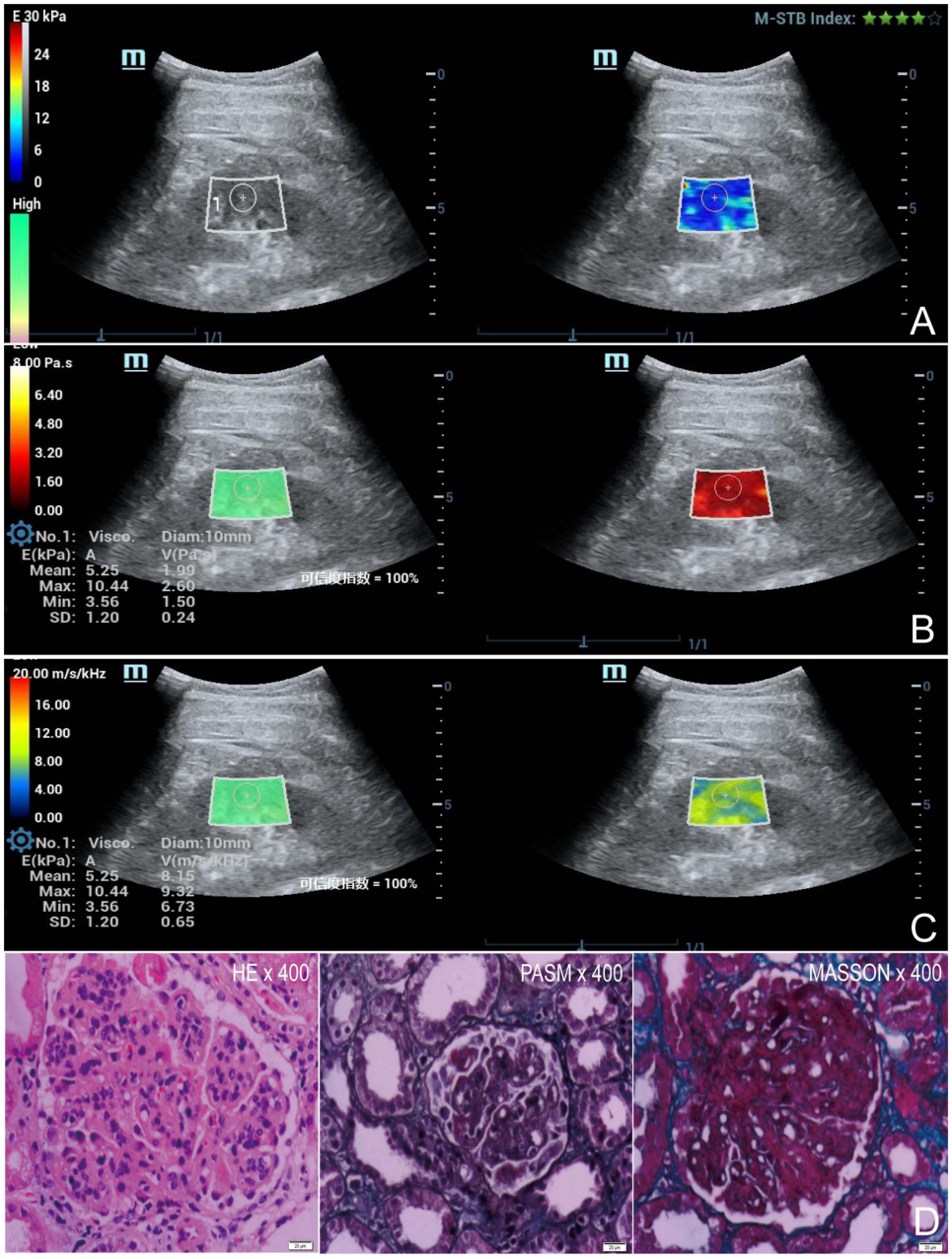

Figure 3 The pathological results were classified as proliferative lupus nephritis of type IV according to ISN/RPS.(**A**). Conventional ultrasound showed that the echo of the renal parenchyma was enhanced. The mean stiffness measured by shear wave elasticity was 7.11 kPa. (**B**). The mean viscosity coefficient measured by viscoelasticity was 2.57 Pa·s. (**C**) The mean dispersion coefficient measured by viscoelasticity was 9.18 m/s/kHz. (**D**) HE staining, PASM staining, and MASSON staining of renal pathology.

Discussion

The results of this study indicated that as a new SWE technology, ultrasonic viscoelastic imaging can effectively and noninvasively evaluate PLN. Vmean was the independent parameter for predicting PLN. When the cutoff value was set at 2.16 Pa·s, we obtained an AUC of 0.77, a sensitivity of 56.7%, and a specificity of 86.8% for predicting PLN. Combining the viscoelastic parameter Vmean with clinical parameters Scr and anti-dsDNA yielded an AUC of 0.83. This study is the first to demonstrate the clinical value of ultrasound viscoelastic imaging for LN evaluation.

This study showed that the viscoelastic parameters (Vmean, Dmean, and Emean) of PLN were significantly greater compared to the control group (all $p < 0.05$). This may have been due to changes in the microstructure of the kidneys in LN patients.[3] Immune complex deposition induces glomerulonephritis and interstitial inflammation, characterized by

https://doi.org/10.2147/JIR.S505223

Table 2 Univariable and Multivariable Analysis of Clinical and Imaging Parameters for Detecting PLN

Characteristic	Univariable Analysis		Multivariable Analysis*	
	Odds Ratio (95% CI)	*p*	Odds Ratio (95% CI)	*p*
Years	0.99 (0.97–1.02)	0.554		
Sex				
Female	0.65 (0.17–2.07)	0.491		
Male	1.53 (0.48–5.82)	0.491		
BMI (kg/m^2)	1.11 (1.0–1.24)	0.062		
Kidney length (cm)	1.23 (0.85–1.80)	0.285		
PSV of interlobar artery (cm/s)	0.97 (0.91–1.03)	0.276		
RI of interlobar artery	6.23 (0.01–5129.93)	0.589		
Emean (kPa)	1.06 (0.90–1.27)	0.497		
Vmean (Pa·s)	83.71 (13.55–724.65)	< 0.001	89.49 (6.50–1878.31)	0.002
Dmean (m/s/kHz)	1.81 (1.26–2.69)	0.002	0.76 (0.41–1.36)	0.367
C3 (g/L)	0.37 (0.10–1.33)	0.13		
C4(g/L)	0.14 (0–5.08)	0.28		
Scr (mg/dL)	15.93 (4.3–79.2)	< 0.001	110.57 (3.14–9329.76)	0.024
Anti-dsDNA (IU/mL)	1.0 (1.0–1.01)	0.04	1.0 (1.0–1.01)	0.015
eGFR(mL/min/1.73m^2)	1.0 (0.99–1)	< 0.001	1.03 (0.99–1.07)	0.175

Notes: *Multivariable logistic regression was performed on the parameters that were statistically significant ($p < 0.05$) in the univariate analysis.

Table 3 Analysis of Performance in Identifying PLN

	AUC	95% CI	Sensitivity (%)	Specificity (%)	Cutoff
Vmean	0.77[ab]	0.69–0.83	56.67	86.79	> 2.16 (Pa·s)
Scr	0.75[ab]	0.67–0.82	77.78	62.26	> 0.68 (mg/dL)
Anti-dsDNA	0.62[a]	0.53–0.70	82.22	39.62	> 33.8 (IU/mL)
Combine	0.83	0.76–0.89	66.89	88.68	> 0.66

Notes: [a]Delong test (1988), compared to Combine, $p < 0.05$. [b]Delong test (1988), compared to AntidsDNA, $p < 0.05$.

mesangial, endothelial, and parietal epithelial cell proliferation, crescent formation, interstitial inflammatory cell infiltration, tubular atrophy, and interstitial fibrosis.[5,9] These abnormalities result in an increase in the elasticity and viscosity of the kidney parenchyma. A recent study on children with glomerular diseases also found that these children had higher kidney parenchymal elasticity and a steeper dispersion slope compared to healthy controls,[25] and our research results were consistent with this finding.

This study revealed that Vmean and Dmean values, indicative of tissue viscosity, varied between the PLN and nPLN groups, potentially due to increased inflammation in PLN. The glomeruli in nPLN are generally normal, with immune complex deposits located in the mesangial area or subepithelium, causing mesangial cell proliferation and expansion of the mesangial area.[3,9] In contrast, PLN is characterized by immune complex deposits in the subendothelium, leading to the proliferation of capillary endothelial cells and mesangial cells, often accompanied by inflammatory cell infiltration and necrotic crescentic lesions.[3,5,9] Consequently, PLN involves a greater number of inflammatory lesions.[26] The inflammatory process can alter the physical properties of tissues.[21,27,28] The infiltration of inflammatory cells, narrowing of intercellular spaces, and stagnation of blood flow increase the internal pressure of organ tissues, leading to an increase in tissue viscosity.[10,29] Previous research indicated that necrotic inflammatory activity markedly elevated dispersion slope values in the liver.[27,30] A recent study on kidney transplantation also discovered that patients with acute kidney injury after transplantation exhibited higher dispersion coefficients and that the overall inflammatory grade was correlated with the dispersion values of the responding tissues.[18]

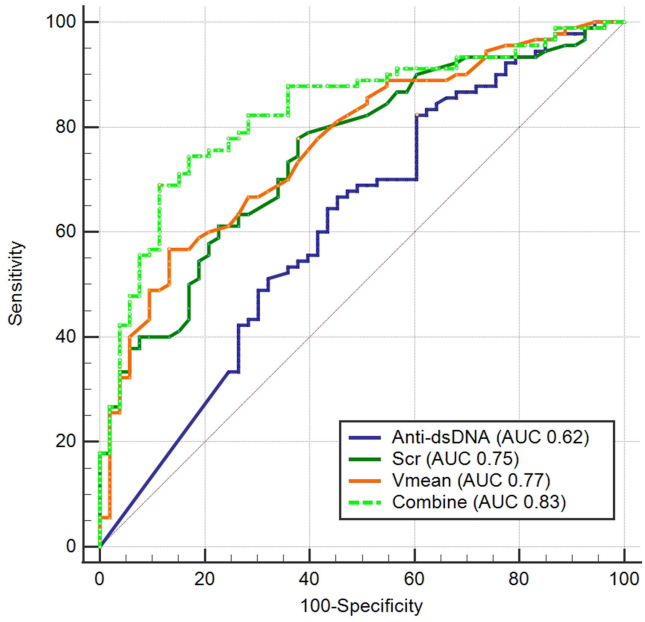

Figure 4 ROC curve for predicting PLN.The AUCs of Vmean, SCr, and anti-dsDNA for predicting PLN were 0.77 (95% CI: 0.69–0.83), 0.75 (95% CI: 0.67–0.82), and 0.62 (95% CI: 0.53–0.70), respectively. The AUC of the combined model was 0.83 (95% CI: 0.76–0.89). The DeLong test revealed that the AUC of the combined model was higher than that of using a single indicator alone. Although there was no significant difference in the AUC between Vmean and Scr, both were higher than the AUC of anti-dsDNA.

Our findings indicate that Vmean, Scr, and Anti-dsDNA are all independent predictors of PLN. Scr is a clinical marker commonly used to assess renal function, while Anti-dsDNA is frequently employed in clinical practice to predict PLN.[31] However, the diagnostic specificity of these two markers decreases in patients with acute kidney injury (AKI) or concurrent autoimmune diseases such as autoimmune vasculitis or mixed connective tissue disease (MCTD).[32] The activity index, based on a semi-quantitative scoring system that takes into account parameters such as interstitial inflammation and leukocyte infiltration, provides a pathological indication of the degree of LN activity and renal

Table 4 The Univariate and Multivariate Analysis of Factors Influencing Vmean

Characteristic	Univariable Analysis		Multivariable Analysis*	
	Odds Ratio (95% CI)	*p*	Odds Ratio (95% CI)	*p*
Years	1.0 (1.0–1.0)	0.724		
Sex				
Female	0.94 (0.80–1.11)	0.473		
Male	1.06 (0.90–1.26)	0.473		
BMI	1.01 (1.0–1.02)	0.197		
Kidney length (cm)	1.01 (0.96–1.07)	0.728		
PSV of interlobar artery (cm/s)	0.99 (0.98–1.0)	0.03	1.0 (0.99–1.0)	0.548
RI of interlobar artery	3.23 (1.24–8.41)	0.018	1.91 (0.93–3.89)	0.079
C3 (g/L)	0.97 (0.80–1.17)	0.735		
C4 (g/L)	1.0 (0.59–1.70)	0.998		
Scr (mg/dL)	1.13 (1.1–1.16)	< 0.001	1.04 (1.0–1.08)	0.077
Anti-dsDNA (IU/mL)	1.0 (1.0–1.0)	0.446		
eGFR(mL/min/1.73m^2)	1.0 (0.99–1)	< 0.001	1.0 (1.0–1.0)	0.087
AI	1.07 (1.06–1.08)	< 0.001	1.05 (1.03–1.06)	< 0.001
CI	1.07 (1.04–1.1)	< 0.001	1.01 (0.99–1.04)	0.247

Notes: *Multivariable logistic regression was performed on the parameters that were statistically significant ($p < 0.05$) in the univariate analysis.

https://doi.org/10.2147/JIR.S505223

Table 5 The Univariate and Multivariate Analysis of Factors Influencing Dmean

Characteristic	Univariable Analysis		Multivariable Analysis*	
	Odds Ratio (95% CI)	*p*	Odds Ratio (95% CI)	*p*
Years	1.0 (0.99–1.02)	0.311		
Sex				
Female	0.62 (0.36–1.07)	0.088		
Male	1.61 (0.93–2.77)	0.088		
BMI	1.07 (1.02–1.12)	0.007	1.05 (1.01–1.09)	0.02
Kidney length (cm)	1.08 (0.90–1.28)	0.425		
PSV of interlobar artery (cm/s)	0.97 (0.94–1.0)	0.045	0.99 (0.97–1.02)	0.619
RI of interlobar artery	2.07 (0.09–50.13)	0.657		
C3 (g/L)	0.76 (0.41–1.41)	0.378		
C4 (g/L)	0.60 (0.11–3.42)	0.57		
Scr (mg/dL)	1.31 (1.18–1.46)	< 0.001	0.96 (0.83–1.11)	0.586
Anti-dsDNA (IU/mL)	1.0 (1.0–1.0)	0.957		
eGFR(mL/min/1.73m^2)	0.99 (0.98–0.99)	< 0.001	0.99 (0.99–1.0)	0.002
AI	1.18 (1.12–1.24)	< 0.001	1.13 (1.06–1.20)	< 0.001
CI	1.13 (1.03–1.24)	0.009	0.96 (0.87–1.05)	0.348

Notes: *Multivariable logistic regression was performed on the parameters that were statistically significant ($p < 0.05$) in the univariate analysis.

Table 6 The Univariate and Multivariate Analysis of Factors Influencing Emean

Characteristic	Univariable Analysis		Multivariable Analysis*	
	Odds Ratio (95% CI)	*p*	Odds Ratio (95% CI)	*p*
Years	0.99 (0.97–1.02)	0.61		
Sex				
Female	1.0 (0.32–3.19)	0.996		
Male	1.0 (0.31–3.17)	0.996		
BMI	0.90 (0.81–0.99)	0.031	0.91 (0.82–1.0)	0.056
Kidney length (cm)	1.11 (0.76–1.61)	0.593		
PSV of interlobar artery (cm/s)	1.08 (1.02–1.15)	0.015	1.07 (1.01–1.14)	0.027
RI of interlobar artery	9.46 (0.01–7875.66)	0.514		
C3 (g/L)	0.63 (0.17–2.33)	0.488		
C4 (g/L)	0.71 (0.02–27.78)	0.856		
Scr (mg/dL)	0.89 (0.70–1.14)	0.364		
Anti-dsDNA (IU/mL)	1.0 (1.0–1.0)	0.509		
eGFR(mL/min/1.73m^2)	1.0 (0.99–1.01)	0.703		
AI	1.02 (0.90–1.01)	0.805		
CI	1.10 (0.90–1.33)	0.353		

Notes: *Multivariable logistic regression was performed on the parameters that were statistically significant ($p < 0.05$) in the univariate analysis.

inflammation, while the chronicity index correlates with renal fibrosis.[9] Our results demonstrated a positive correlation between Vmean and activity index as well as chronicity index ($r = 0.57$ and $r = 0.34$, respectively, $p < 0.05$), indicating that ultrasonic viscoelastic parameters can reflect the degree of tissue inflammatory infiltration and fibrosis severity. Relevant studies have also demonstrated that ultrasound shear wave viscosity parameters can non-invasively identify lobular inflammation and fibrosis in patients with non-alcoholic fatty liver disease (NAFLD).[33] A study on liver transplants further revealed that the shear wave dispersion slope correlates with the degree of necroinflammation and fibrosis.[17] Therefore, combining the ultrasound viscosity parameter Vmean with laboratory markers such as Scr and Anti-

dsDNA can significantly enhance the diagnostic efficacy for PLN, outperforming individual indicators in predictive performance (AUC = 0.83) while markedly improving diagnostic specificity.

Multivariate analysis showed that factors affecting Vmean and Dmean were correlated with the activity index ($p < 0.05$), and correlation analysis revealed that the activity index was significantly positively correlated with both Vmean ($r = 0.57$, $p < 0.001$) and Dmean ($r = 0.43$, $p < 0$ 0.001). Our findings align with prior research indicating that tissue viscosity, rather than tissue elasticity, is associated with inflammatory activity.[17,21,27]

In addition to the activity index, we also found that eGFR and BMI were factors that influenced the Dmean values. In a study using viscous plane wave ultrasound (Vi PLUS) to assess renal viscosity in healthy individuals, viscosity had a negative correlation with BMI and a positive correlation with eGFR.[34] This contradicts our research findings showing a positive correlation between Dmean and BMI ($r = 0.25$, $p = 0.003$), and a negative correlation between Dmean and eGFR ($r = -0.44$, $p < 0.001$). However, that research was conducted on healthy individuals with normal renal function, and it did not involve people with abnormal renal function. Our research subjects were LN patients, and the activity index was a factor affecting Dmean, which may have affected the influence of BMI and eGFR on Dmean. Additionally, the ultrasonic equipment we used differed, which may have led to discrepancies in the calculation of the tissue viscosity coefficients. In our study, the dispersion coefficient (Dmean) was calculated based on SWD imaging. SWD employs a simple linear fitting relationship to indirectly reflect the viscosity of tissues.[16,35] This could indeed be one of the reasons for the discrepancies in our research results.

The PSV of the interlobar artery significantly affected the Emean value in our study (OR = 1.07, $p = 0.027$). Kidney hemodynamics are potential factors affecting kidney elasticity.[35] As a highly vascularized organ, the kidney receives approximately 25% of the cardiac output.[15] Studies have shown that reduced blood flow slows the propagation velocity of shear waves, leading to a decrease in elasticity measurements.[36,37] Liu et al found that shear wave propagation velocity and elasticity measurements increased with increases in organ blood perfusion pressure.[38] Our research results also confirmed that blood flow affects kidney elasticity measurements.

Ultrasound viscoelastic imaging, as a new technique within the category of shear wave elastography, depends heavily on the technical skills of the operating physician for the accuracy and reliability of its results. In this study, we established strict quality control standards and operational procedures. The intraobserver and interobserver consistency showed that the consistency coefficients were no less than 0.8, indicating that viscoelastic imaging has excellent reproducibility.

The current research has some shortcomings. First, this was a prospective, single-center study, and the exclusion of patients with type VI LN in this study may have resulted in selection bias. Future researchers should use larger sample sizes and conduct multi-center validation studies to better understand the potential of this noninvasive technology for diagnosing and treating LN. Second, no comparative study has considered each pathological type of LN. Consequently, the applicability of viscoelastic imaging to different pathological types remains unknown.

In conclusion, ultrasonic viscoelastic imaging, as a noninvasive examination method, can predict PLN by quantitatively measuring the viscosity of tissues.

Data Sharing Statement

All de-identified participant data from this study can be provided upon request by contacting the corresponding author.

Disclosure

The authors report no conflicts of interest in this work.

References

1. Kiriakidou M, Ching CL. Systemic lupus erythematosus. *Ann Intern Med*. 2020;172:C81–C96. doi:10.7326/AITC202006020
2. Barber M, Drenkard C, Falasinnu T, et al. Global epidemiology of systemic lupus erythematosus. *Nat Rev Rheumatol*. 2021;17:515–532. doi:10.1038/s41584-021-00668-1
3. Yu C, Li P, Dang X, Zhang X, Mao Y, Chen X. Lupus nephritis: new progress in diagnosis and treatment. *J Autoimmun*. 2022;132:102871. doi:10.1016/j.jaut.2022.102871
4. KDIGO. 2021 clinical practice guideline for the management of glomerular diseases. *Kidney Int*. 2021;100:S1–S276. doi:10.1016/j.kint.2021.05.021
5. Weening JJ, D'Agati VD, Schwartz MM, et al. The classification of glomerulonephritis in systemic lupus erythematosus revisited. *Kidney Int*. 2004;65:521–530. doi:10.1111/j.1523-1755.2004.00443.x

6. Fanouriakis A, Kostopoulou M, Cheema K, et al. 2019 update of the joint European league against rheumatism and European renal association-European dialysis and transplant association (EULAR/ERA-EDTA) recommendations for the management of lupus nephritis. *Ann Rheum Dis*. 2020;79:713–723. doi:10.1136/annrheumdis-2020-216924
7. Rovin BH, Ayoub IM, Chan TM, et al. Executive summary of the KDIGO 2024 clinical practice guideline for the management of lupus nephritis. *Kidney Int*. 2024;105:31–34. doi:10.1016/j.kint.2023.09.001
8. Gasparotto M, Gatto M, Binda V, Doria A, Moroni G. Lupus nephritis: clinical presentations and outcomes in the 21st century. *Rheumatology (Oxford)*. 2020;59:v39–v51. doi:10.1093/rheumatology/keaa381
9. Bajema IM, Wilhelmus S, Alpers CE, et al. Revision of the international society of nephrology/renal pathology society classification for lupus nephritis: clarification of definitions, and modified national institutes of health activity and chronicity indices. *Kidney Int*. 2018;93:789–796. doi:10.1016/j.kint.2017.11.023
10. Razek A, Khalek A, Tharwat S, Nassar MK, Tharwat N. Diffusion tensor imaging of renal cortex in lupus nephritis. *Jpn J Radiol*. 2021;39:1069–1076. doi:10.1007/s11604-021-01154-0
11. Kang ES, Ahn SM, Oh JS, et al. Risk of bleeding-related complications after kidney biopsy in patients with systemic lupus erythematosus. *Clin Rheumatol*. 2023;42:751–759. doi:10.1007/s10067-022-06394-7
12. Cao H, Ke B, Lin F, Xue Y, Fang X. Shear wave elastography for assessment of biopsy-proven renal fibrosis: a systematic review and meta-analysis. *Ultrasound Med Biol*. 2023;49:1037–1048. doi:10.1016/j.ultrasmedbio.2023.01.003
13. Mo XL, Meng HY, Wu YY, Wei XY, Li ZK, Yang SQ. Shear wave elastography in the evaluation of renal parenchymal stiffness in patients with chronic kidney disease: a meta-analysis. *J Clin Med Res*. 2022;14:95–105. doi:10.14740/jocmr4621
14. Sigrist R, Liau J, Kaffas AE, Chammas MC, Willmann JK. Ultrasound elastography: review of techniques and clinical applications. *Theranostics*. 2017;7:1303–1329. doi:10.7150/thno.18650
15. Lubas A, Kade G, Saracyn M, Niemczyk S, Dyrla P. Dynamic tissue perfusion assessment reflects associations between antihypertensive treatment and renal cortical perfusion in patients with chronic kidney disease and hypertension. *Int Urol Nephrol*. 2018;50:509–516. doi:10.1007/s11255-018-1798-9
16. Lim W, Ooi EH, Foo JJ, Ng KH, Wong J, Leong SS. The role of shear viscosity as a biomarker for improving chronic kidney disease detection using shear wave elastography: a computational study using a validated finite element model. *Ultrasonics*. 2023;133:107046. doi:10.1016/j.ultras.2023.107046
17. Lee DH, Lee JY, Bae JS, et al. Shear-wave dispersion slope from US shear-wave elastography: detection of allograft damage after liver transplantation. *Radiology*. 2019;293:327–333. doi:10.1148/radiol.2019190064
18. Kim TM, Ahn H, Cho JY, et al. Prediction of acute rejection in renal allografts using shear-wave dispersion slope. *Eur Radiol*. 2023;34:4527–4537. doi:10.1007/s00330-023-10492-8
19. Stoian D, Borlea A, Sporea I, Popa A, Moisa-Luca L, Popescu A. Assessment of thyroid stiffness and viscosity in autoimmune thyroiditis using novel ultrasound-based techniques. *Biomedicines*. 2023;12:11. doi:10.3390/biomedicines12010011
20. Jia W, Xia S, Jia X, et al. Ultrasound viscosity imaging in breast lesions: a multicenter prospective study. *Acad Radiol*. 2024;31:3499–3510. doi:10.1016/j.acra.2024.03.017
21. de Araujo NJ. Shear-wave dispersion slope: do we have the tool for detecting necroinflammation? *Radiology*. 2020;294:483–484. doi:10.1148/radiol.2019192326
22. Yuan H, Huang Q, Wen J, Gao Y. Ultrasound viscoelastic imaging in the noninvasive quantitative assessment of chronic kidney disease. *Ren Fail*. 2024;46:2407882. doi:10.1080/0886022X.2024.2407882
23. Delanaye P, Masson I, Maillard N, Pottel H, Mariat C. The New 2021 CKD-EPI equation without race in a European cohort of renal transplanted patients. *Transplantation*. 2022;106:2443–2447. doi:10.1097/TP.0000000000004234
24. Mellema DC, Song P, Kinnick RR, et al. Probe oscillation shear elastography (PROSE): a high frame-rate method for two-dimensional ultrasound shear wave elastography. *IEEE Trans Med Imaging*. 2016;35:2098–2106. doi:10.1109/TMI.2016.2550007
25. Yao S, Cai Y, Hu S, et al. The value of shear wave elasticity and shear wave dispersion imaging to evaluate the viscoelasticity of renal parenchyma in children with glomerular diseases. *Bmc Nephrol*. 2023;24:306. doi:10.1186/s12882-023-03357-1
26. Kwon OC, Park JH, Park HC, et al. Non-histologic factors discriminating proliferative lupus nephritis from membranous lupus nephritis. *Arthritis Res Ther*. 2020;22:138. doi:10.1186/s13075-020-02223-x
27. Sugimoto K, Moriyasu F, Oshiro H, et al. Clinical utilization of shear wave dispersion imaging in diffuse liver disease. *Ultrasonography*. 2020;39:3–10. doi:10.14366/usg.19031
28. Chen S, Urban MW, Pislaru C, et al. Shearwave dispersion ultrasound vibrometry (SDUV) for measuring tissue elasticity and viscosity. *IEEE Trans Ultrason Ferroelectr Freq Control*. 2009;56(1):55–62. doi:10.1109/TUFFC.2009.1005
29. Vasconcelos L, Kijanka P, Grande JP, et al. Kidney cortex shear wave motion simulations based on segmented biopsy histology. *Comput Methods Programs Biomed*. 2024;245:108035. doi:10.1016/j.cmpb.2024.108035
30. Sugimoto K, Moriyasu F, Oshiro H, et al. Viscoelasticity measurement in rat livers using shear-wave US Elastography. *Ultrasound Med Biol*. 2018;44:2018–2024. doi:10.1016/j.ultrasmedbio.2018.05.008
31. Fava A, Wagner CA, Guthridge CJ, et al. Association of autoantibody concentrations and trajectories with lupus nephritis histologic features and treatment response. *Arthritis Rheumatol*. 2024;76:1611–1622. doi:10.1002/art.42941
32. Zhao X, Wen Q, Qiu Y, Huang F. Clinical and pathological characteristics of ANA/anti-dsDNA positive patients with antineutrophil cytoplasmic autoantibody-associated vasculitis. *Rheumatol Int*. 2021;41:455–462. doi:10.1007/s00296-020-04704-3
33. Jang JK, Lee ES, Seo JW, et al. Two-dimensional shear-wave elastography and us attenuation imaging for nonalcoholic steatohepatitis diagnosis: a cross-sectional, multicenter study. *Radiology*. 2022;305:118–126. doi:10.1148/radiol.220220
34. Maralescu FM, Bende F, Sporea I, et al. Non-invasive evaluation of kidney elasticity and viscosity in a healthy cohort. *Biomedicines*. 2022;11:10. doi:10.3390/biomedicines11010010
35. Lim W, Ooi EH, Foo JJ, Ng KH, Wong J, Leong SS. Shear wave elastography: a review on the confounding factors and their potential mitigation in detecting chronic kidney disease. *Ultrasound Med Biol*. 2021;47:2033–2047. doi:10.1016/j.ultrasmedbio.2021.03.030
36. Ipek-Ugay S, Tzschatzsch H, Braun J, Fischer T, Sack I. Physiologic reduction of hepatic venous blood flow by the valsalva maneuver decreases liver stiffness. *J Ultrasound Med*. 2017;36:1305–1311. doi:10.7863/ultra.16.07046

37. Chen Y, Li J, Zhou Q, Lyu G, Li S. Detection of liver and spleen stiffness in rats with portal hypertension by two-dimensional shear wave elastography. *Bmc Med Imaging*. 2022;22:68. doi:10.1186/s12880-022-00786-6
38. Liu X, Li N, Xu T, et al. Effect of renal perfusion and structural heterogeneity on shear wave elastography of the kidney: an in vivo and ex vivo study. *Bmc Nephrol*. 2017;18:265. doi:10.1186/s12882-017-0679-2